Preparation of a novel sludge-derived biochar by K_2FeO_4 conditioning to enhance the removal of Pb^{2+}

Junsen Wang [a], Tianrun Wang [a], Qinyun Zhu [a], Shike Zhang [a], Qi Shi [a], Jean-Marc Chovelon [c], Hongtao Wang [a,b,*]

[a] College of Environmental Science and Engineering, Key Laboratory of Yangtze River Water Environment, Ministry of Education, Tongji University, Siping Rd 1239, Shanghai 200092, China
[b] Shanghai Institute of Pollution Control and Ecological Security, UNEP-TONGJI Institute of Environment for Sustainable Development, Shanghai 200092, China
[c] IRCELYON, CNRS UMR 5256, Université Claude Bernard Lyon 1, 2 avenue Albert-Einstein, F-69626 Villeurbanne, France

ARTICLE INFO

ABSTRACT

In this study, three types of sludge-derived biochars (BC1, BC2 and BC3) were prepared by 1) original sludge, 2) sludge after K_2FeO_4 conditioning, and 3) sludge after acidification + K_2FeO_4 conditioning. The results show that the biochar prepared from the conditioned sludge has additional functional groups, and its Pb^{2+} removal effect is greatly enhanced. The concentration of Pb^{2+} in the effluent can be reduced to <0.06 μg/L. The original sludge-derived biochar can only remove at most 58.02% of Pb^{2+}. The maximum adsorption capacity of BC3 is six times greater than that of BC1. The ion exchange effect of Ca^{2+} and Mg^{2+} on the biochar surface and the complexation of free -OH or -COOH functional groups lead to an excellent adsorption effect on Pb^{2+}. The sludge-derived biochar prepared after the conditioning of K_2FeO_4 can realize efficient removal of Pb^{2+}, providing new initiatives for subsequent sludge resource utilization.

1. Introduction

Sludge has a high yield as a byproduct of sewage treatment worldwide. As of 2015, sludge production in the United States (US) increased to 8 million tons/year. It was expected that by 2020 sewage sludge production in Europe can reach approximately 13 million tons/year (dry solids), while in China, it can reach around 60 million tons/year [1]. Many countries, such as China and the European Union (EU), face pressure for improved sludge treatment and disposal [2–4]. The use of dehydrated sludge to prepare biochar has received much attention in the field of sludge resource utilization. Sludge-derived biochar is a carbon-rich solid adsorbent with rich functional groups, so it has a large number of exchangeable ions and surface adsorption sites, which can effectively remove pollutants in water [5,6].

Lead is a persistent pollutant that is toxic to many organisms. It has been confirmed to have toxic effects on the human nervous, cardiovascular, skeletal, reproductive, and immune systems [7]. Therefore, effective, economical, and convenient methods are needed to eliminate excess lead in water. Ion exchange [8], chemical precipitation [9],

flocculation [10], and adsorption [11] have been applied to remove heavy metals, including lead [12]. Among them, the adsorption method may be a low-cost and straightforward operation that can efficiently remove low-concentration lead in the solution [13]. As an adsorbent, sludge-derived biochar can be used to remove Pb^{2+} from water. For example, some researchers have successfully prepared a new type of amino-functionalized magnetic aerobic granular sludge biochar through magnetization modification and used it for the adsorption of Pb^{2+} in the aqueous phase [14].

Sludge must be dewatered before preparing sludge-derived biochar, and pretreatment before sludge dewatering usually is necessary. Sludge oxidation is gradually becoming a research hotspot in a sludge dewatering pretreatment, since in addition to improve the dewatering performance, it also has a significant effect on sludge deodorization [15]. In recent years, K_2FeO_4, a highly efficient and versatile green oxidant commonly used in drinking water treatment [16], has gained new consideration in the field of sludge treatment. For example, Wu et al. [17] utilized sludge biochar and ferrate to condition sludge synergistically. In addition, some studies combine K_2FeO_4 with ultrasonic and

alkalization technology to decompose sludge and improve its dehydration effect [18]. K_2FeO_4 is a strong oxidant, and the standard electrode potential under acidic conditions is as high as +2.20 V, which can oxidize the organic matter and extracellular polymeric substances (EPS) in the sludge and release bound water [19]. Comparatively, the reduction product Fe^{3+} generated *in situ* during the oxidation process of FeO_4^{2-} is a common coagulant that has the effect of adsorption and charge neutralization and compresses the electric double layer [15]. Although studies exist on sludge treatment with K_2FeO_4, only few of them dealt with the preparation of sludge-derived biochar after K_2FeO_4 conditioning.

In this study, three types of sludge-derived biochar (named as BC1, BC2, BC3) for the removal of Pb^{2+} in water were prepared, *viz.*, raw sludge, sludge after K_2FeO_4 conditioning, and sludge after an acidification step + K_2FeO_4 conditioning. The study aims to (1) prepare a new type of sludge-derived biochar by acidification and K_2FeO_4 conditioning to adsorb Pb^{2+} in water and (2) research the elimination effect of the three biochars on Pb^{2+} in water and reveal the adsorption mechanism. Therefore, this study proposes a new way to utilize sludge as a resource and develops a new type of adsorbent to treat Pb^{2+} in water.

2. Materials and methods

2.1. Biochar preparation

The sludge treated in this experiment was taken from the Quyang Sewage Treatment Plant's secondary sedimentation tank in Shanghai. The sludge was stored in a refrigerator at 4 °C to ensure the original sludge's basic properties. It was thoroughly shaken before use, and all experiments were completed within 4 days.

The original sludge, K_2FeO_4 conditioned sludge, acidification, and K_2FeO_4 oxidation combined treatment sludge biochar were prepared (Supplementary Material (SM), Fig. S1) to reflect the physical and chemical property improvements of the biochar after conditioning. The original sludge was conditioned and dewatered by a cloth filter press. These samples were removed from the filter bag and placed in an 80 °C blast oven to dry to constant weight. The samples were then placed in a ceramic crucible and put in a tube furnace, set to 550 °C at a heating rate of 5 °C/min, kept for 4 h, cooled down naturally, passed through a 60-mesh sieve, and stored for use as BC1. At the initial stage, K_2FeO_4 solid was added into the second sludge group before sludge dewatering at approximately 10% of dry sludge mass, and after full shaking to ensure complete dissolution, the reaction took 30 min. The subsequent experimental operations were the same as all steps of No. 1 experimental biochar production. The No. 3 sludge group was first treated by sulfuric acid to adjust its pH to 2, then 10% content of the dry basis potassium ferrate solid was added before sludge dewatering. The remaining steps were the same as those in experiment No. 2 (SM, Fig. S1).

2.2. Adsorption experiments

At pH = 2, 3, 4, and 5, the initial concentration of Pb^{2+} used was 100 mg/L, and the dosage of sludge-derived biochar was 5 g/L. After stirring with a magnetic stirrer for 24 h to ensure adsorption equilibrium, the supernatant was passed through a 0.22 μm filter membrane to determine the Pb^{2+} concentration. Under the optimal pH conditions, with the same initial concentration of Pb^{2+} and biochar quantity, the Pb^{2+} concentration was measured at 0, 5, 10, 20, 40, 60, 90, and 120 min. The results were employed for the study of adsorption kinetics.

2.3. Adsorption mechanism

2.3.1. Experimental equipment

The specific surface areas of biochar were determined by an accelerated surface area and porosimetry system (BET, ASAP 2020, USA). The measurement conditions were as follows: the sample was dried under

Table 1
Characteristics of three sludge-based biochars (BC1, BC2, and BC3).

Sample	BC1	BC2	BC3
Leachate pH	8.75	9.67	9.08
Specific surface area/$m^2 \cdot g^{-1}$	8.66	7.90	6.87
Pore volume/$cm^3 \cdot g^{-1}$	0.0754	0.0771	0.0768
C/%	25.42	24.62	23.57
N/%	3.85	3.56	3.26
H/%	1.69	1.514	1.303
S/%	0.318	0.987	0.986

dynamic vacuum at 150 °C for 6 h and then subjected to nitrogen adsorption and desorption measurements. The capillary suction time (CST) of sludge was verified by a Triton UA CST measuring instrument (304 M), and the size of CST filter paper is 7 × 9 cm. A SU8010 scanning electron microscopy energy-dispersive X-ray spectroscopy (SEM-EDS; Hitachi, Japan) was used to examine the material's surface morphologies and element distribution. Moreover, Fourier transform infrared spectroscopy (FTIR) images were assessed *via* a TENSOR 37 spectrometer (Bruker, Germany) with a wavelength of 400–4000 cm^{-1} to identify the surface functional groups of biochars. Additionally, X-ray diffraction (XRD) analysis was applied to evaluate the biochar phases *via* a D8 Advance instrument (Bruker, Germany). An organic element analyzer (vario Micro cube) was employed to define the C/H/N/S content of the three biochar samples. Lastly, sludge pyrolysis was performed in a Junke tube furnace (JGF1200-120, China), and the Pb^{2+} concentration was measured by inductively coupled plasma optical emission spectroscopy (ICP-OES; Perkin Elmer, Optima 2100 DV, USA) (1–10 μg/L) or inductively coupled plasma mass spectrometry (ICP-MS; Agilent, 7700, USA) (<1 μg/L).

2.3.2. Functional group blocking

A functional group blocking experiment was implemented according to the method reported by Chen and Yang (2006) [20]. The experiment explored the role of hydroxyl and carboxyl groups, which used methanol and formaldehyde to block free -COOH and -OH on the surface (see SM, Text S1 for detailed steps). According to the literature [20,21], formaldehyde can react with an alcoholic group to form a firmly linked structure, and the carboxyl group can also be modified with methanol at acidic conditions:

$$2R - OH + HCHO \rightarrow (R - O)_2CH_2 + H_2O \tag{1}$$

$$AC(O)OH + CH_3OH \rightarrow AC(O)OCH_3 + H_2O \tag{2}$$
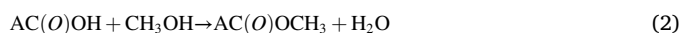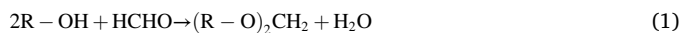
Previous studies have shown that the blocking technique does not alter the adsorbent's surface charge or significantly impact its leaching solution pH [22]. Therefore, the process does not affect ion exchange or other properties.

2.4. Adsorption kinetics and isotherms

This study attempts to use the pseudo-first-order and the pseudo-second-order kinetic models for correlation fitting analysis. See SM, Text S2 for details. The most commonly used adsorption isotherms (Langmuir and Freundlich adsorption isotherms) were adopted in this research (SM, Text S3).

2.5. Leaching experiment

The acetic acid buffer solution was used as the extractant to simulate the leaching of harmful components. The primary sludge disposal method are sanitary landfills. Therefore, this system was chosen to evaluate the environmental leaching risk of sludge-derived biochar after Pb^{2+} adsorption. The detailed steps are in SM, Text S4.
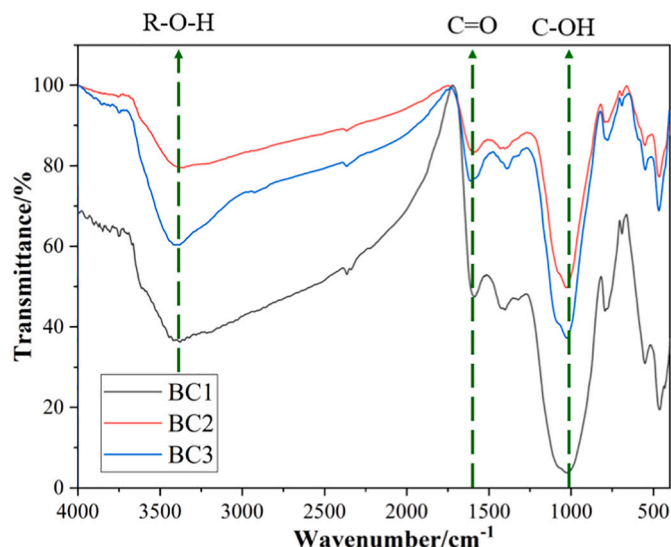
Fig. 1. The FT-IR spectra of 3 kinds of biochars (BC1, BC2, and BC3).

## 3. Results and discussion

3.1. Basic properties of biochar

The pH and specific surface area of the biochar leachding solution are presented in Table 1.

It can be seen from Table 1 that the carbon (C) content of the three types of sludge-derived biochar is relatively high. BC2 contains K_2FeO_4, and the dissolved K_2FeO_4 is alkaline; therefore, its pH was higher than that of biochar BC1, and BC3 has a lower pH than BC2. As a result, an acidification step was included. The leaching fluids of the three adsorbent materials in this experiment are weakly alkaline, similar to the fact that most biochars obtained by Yuan et al. are naturally alkaline [23]. In summary, the three sludge-derived biochars do not remove Pb^{2+} in water simply by alkali precipitation [24].

Table 1 shows that specific surface areas (<9 $m^2 \cdot g^{-1}$) and pore volumes of the adsorbent materials are low. The Fourier transform infrared spectrum of biochar based on the air background is displayed in Fig. 1. Consequently, the peaks from 3620 cm^{-1}, 3422 cm^{-1}, 1620 cm^{-1}, and 1030 cm^{-1} in the spectrum demonstrate the free OH, R-O-H, C=O, and C-OH group stretching vibrations, respectively. The biochar functional groups are essentially the same. The FTIR absorption peak reveals the presence of hydroxyl and carboxyl groups, and these functional groups can be deprotonated in the form of proton donors to participate in the removal of Pb^{2+} [25]. On the other hand, Fig. 1 indicated that the
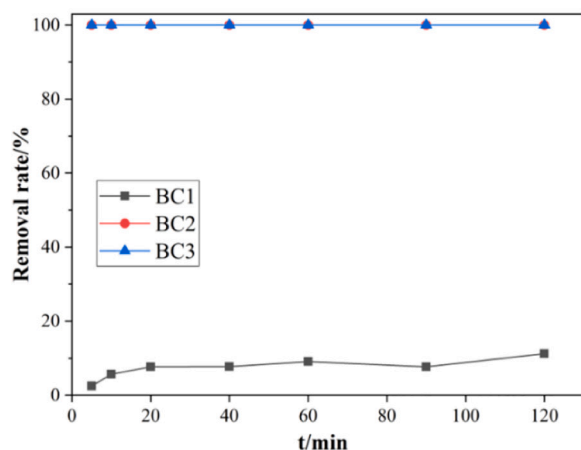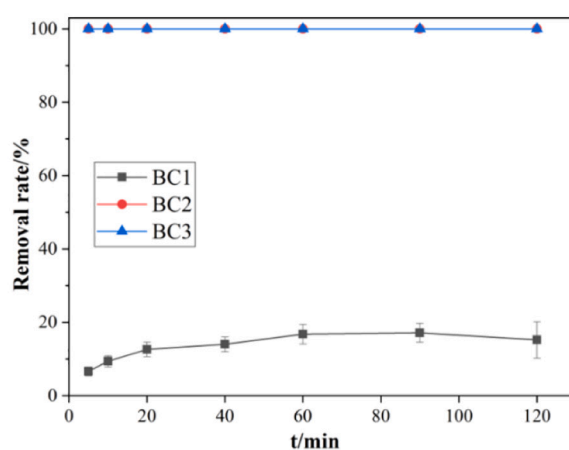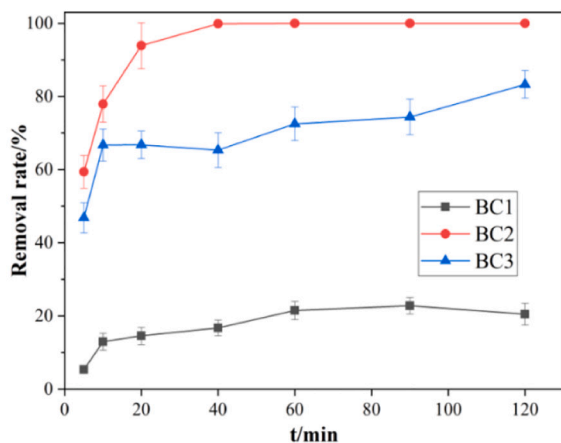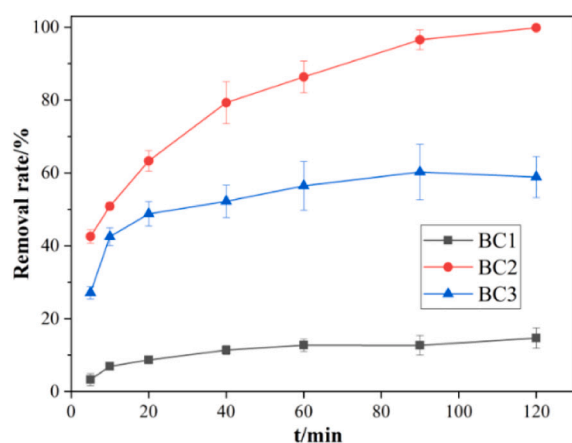

Fig. 2. Various Pb^{2+} removal rates at pH = 3 as a function of time: (a) 1 mg/L, (b) 25 mg/L, (c) 75 mg/L, and (d) 100 mg/L.

functional group abundance of BC2 is the highest, followed by BC3 and BC1. This indicates that the addition of K_2FeO_4 promotes the formation of more functional groups on the surface of the pyrolysis product, which is more conducive to the removal of Pb^{2+}. Therefore, ion exchange effects, functional groups, and other influences were studied to investigate the mechanisms.

The SEM analysis of the three biochars is shown in SM, Fig. S3. It is observed that the surfaces of the three carbons are dense, and do not show a clear porous structure, which is consistent with the lower specific surface area.

3.2. Adsorption effect

3.2.1. Effect of pH

pH is an important parameter that affects the adsorption process. The initial pH range set in this experiment was 2–5, and the initial concentration of Pb^{2+} was 100 mg/L. Complete adsorption was achieved over a period of 24 h. The specific experimental results are exhibited in SM, Fig. S2.

Under various pH conditions, the removal effect of BC2 is found to be superior, BC3 is second-best, and BC1 is lower than both. The findings confirmed that the biochar prepared by sludge conditioning with K_2FeO_4 was considerably better in removing pollutants. Moreover, the concentration of Pb^{2+} in the effluent after the adsorption of BC2 biochar at pH = 3, 4, and 5 was lower than the detection limit of ICP-MS (0.06 μg/L), and the concentration of Pb^{2+} in the effluent of BC3 biochar adsorbed at pH = 3, 4, and 5 was lesser than 7 μg/L, indicating that the two sludge-derived biochars conditioned by K_2FeO_4 exhibited trace amounts of Pb^{2+} removal capacity.

Furthermore, when the initial pH is 4 or 5, the three biochars can remove 100 mg/L of Pb^{2+} within 120 mins. However, when the pH dropped to 2 or 3, the removal rate of Pb^{2+} by BC1 and BC3 decreased substantially. At pH = 2, the removal rates of Pb^{2+} by BC1 and BC3 biochar were only 58.02% and 78.52%, respectively. In contrast, BC2 can eradicate 99.18% of Pb^{2+} even under the strong acid condition of pH = 2, signifying a high acid resistance. This is likely because BC2 has a larger abundance of functional groups such as hydroxyl and carboxyl groups (Fig. 1), which provides more opportunities for complexation [25]. At the same time, the leaching solution of BC2 is significantly more alkaline than the other two biochars, indicating that it can better neutralize the acidity of the environments to a certain extent, and promote the adsorption of lead ions.

Pb^{2+} can be eliminated by simple alkaline precipitation at higher pH, and it is more difficult to remove heavy metals under acidic conditions. To ensure the BC1 biochar has a specific adsorption effect for subsequent analysis, we chose pH 3 as the pH condition for succeeding experiments in this study.

3.2.2. Adsorption kinetics

The effect of contact time on Pb^{2+} adsorption onto biochars is shown Fig. 2 for the following Pb^{2+} concentrations: 1, 25, 75, and 100 mg/L.

According to Fig. 2a and b, for 1 mg/L and 25 mg/L initial concentrations of Pb^{2+}, <5 min is required for BC2 and BC3 to remove Pb^{2+} from the solution (removal rate close to 100%), whereas the removal capacity of Pb^{2+} by BC1 is poor.

When the initial concentration of Pb^{2+} is 75 or 100 mg/L (Fig. 2c and d), the removal rates of Pb^{2+} by BC1 and BC3 biochar are limited within 120 min, and BC2 performs much better than BC1 and BC3. From Fig. S2, it is evident that BC2 can effectively remove 100 mg/L Pb^{2+} at pH 2–5, whereas the efficiency of BC1 and BC3 is much lower at pH 2. Even though BC1 and BC3 can reach high removal rates of Pb^{2+} at pH 3 and 24 h (Fig. S2), their removal rates of Pb^{2+} at 120 min are very low (Fig. 2d).

In summary, the original sludge-derived biochar is not ideal for the adsorption of low-concentration Pb^{2+}. The two sludge-derived biochar types conditioned by K_2FeO_4 exhibited a high removal capacity of trace

Table 2
The maximum adsorption capacity of several materials for Pb^{2+} removal.

Material	Adsorption pH	Maximum adsorption capacity/mg·g^{-1}	References
Nano-TiO$_2$ Immobilized on Silica Gel	5	3.16	[28]
Melamine-grafted chitosan	5	19.96	[29]
The seed husk of *Calophyllum inophyllum*	4	34.5	[30]
APTES functionalized magnetic biochar	6.8	64.92	[31]
CMC-MMT organic-inorganic Hybrid composite	5	82.4	[32]
Sludge-based biochar	5	57.48	[33]
Resource utilization of swine sludge to prepare modified biochar	5 ± 0.3	145	[34]
Pyrolysis of sewage sludge by electromagnetic induction	6–7	116.2	[35]
BC1 Biochar	3	5.71	This study
BC2 Biochar	3	24.1	This study
BC3 Biochar	3	36.1	This study

Pb^{2+} for the adsorption of high-concentration Pb^{2+}. Among them, BC2 has dramatically increased the adsorption rate under the premise of ensuring the adsorption effect.

According to the adsorption results of Fig. 2, the $\log(q_e-q_t)$ and t/q_t values of each time node were calculated, and a fitting analysis of the pseudo-first-order and pseudo-second-order kinetic model was performed.

The fitting parameters were calculated, and the results are summarized in SM, Table S1. Based on the above table, the adsorption kinetic experimental findings of this research have a high degree of fitting with the pseudo-second-order kinetic model. The R^2 values of the three biochars are all >0.99. The theoretical equilibrium adsorption capacities (q_e) obtained from the model are 2.881 mg/g, 20.747 mg/g, and 12.706 mg/g for BC1, BC2, and BC3, respectively. Moreover, the fitting accuracy of the pseudo-first-order kinetic model is low, and the theoretical equilibrium adsorption capacity is different from the experimental value, so it is not suitable for this experiment. In summary, the pseudo-second-order kinetic model is a theoretical model applicable to this material's adsorption kinetics.

3.2.3. Adsorption isotherm

According to the adsorption results, the C_e and q_e values can be computed and used for fitting analysis performed with Langmuir and Freundlich adsorption isotherms.

The calculated fitting parameters and the results are summarized in SM, Table S2. The Langmuir adsorption isotherm is well fitted to this experiment, with R^2 values >0.99. The Freundlich adsorption isotherm is not suitable for this experiment, implying that Pb^{2+} is covered in a single layer on the biochar surface. From the Langmuir adsorption isotherm simulation results, the theoretical maximum adsorption capacity (q_{max}) of the three sludge-derived biochar materials can be obtained. This is an essential parameter of the adsorption material, which can directly reflect the material's removal capacity and is the same as other standards for material comparison. The three materials' maximum adsorption capacities are 5.71 mg/g, 24.1 mg/g, and 36.1 mg/g for BC1, BC2, and BC3, respectively. The maximum adsorption capacity order is different from the theoretical equilibrium adsorption capacity for the three materials obtained by the adsorption kinetics, signifying that the removal rate of Pb^{2+} is higher for BC2. Simultaneously, BC3 has a robust ability to deal with high concentrations of Pb^{2+} in the adsorption saturation state. In short, whether it is adsorption kinetics or thermodynamics, the adsorption performance of the biochar material prepared by the K_2FeO_4 conditioned sludge is much improved compared to the original sludge-derived biochar.
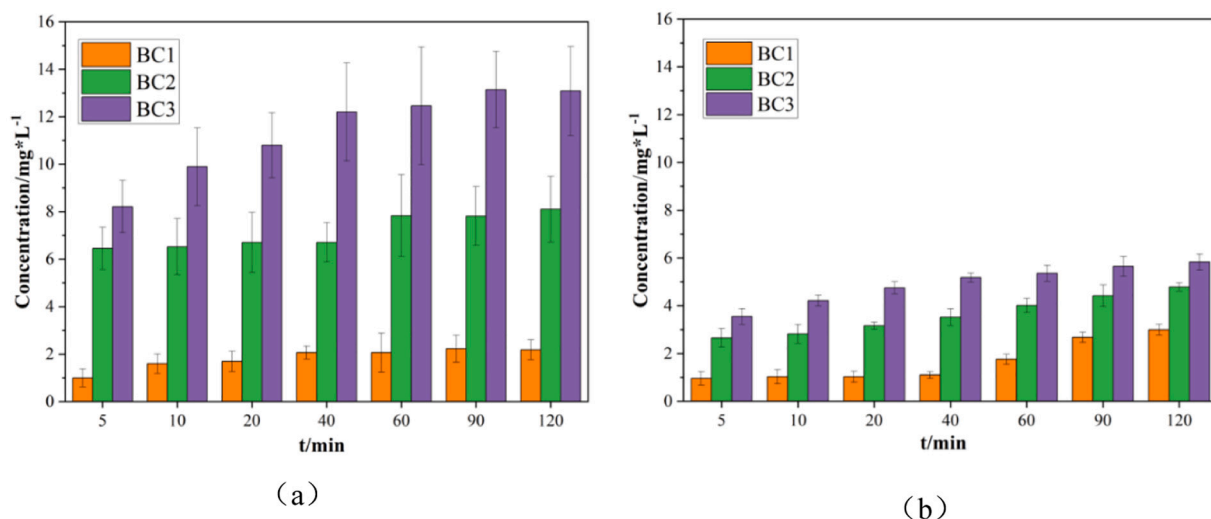
Fig. 3. Variation of(*a*)Ca^{2+} and(*b*)Mg^{2+} concentrations with time.

3.2.4. Comparison with other materials

It was reported that the specific surface areas of adsorbent activated carbon can reach 1940 $m^2 \cdot g^{-1}$ [26], and those of silica gel can reach 82–100 $m^2 \cdot g^{-1}$. The specific surface area and pore volume of the adsorbent material in this experiment are much lower than those of the general adsorbents (Table 1), proving that the three sludge-derived biochars do not efficiently eliminate Pb^{2+} in water through a simple physical adsorption process. This outcome is likely related to the original sludge and the biochar's preparation process. At the same time, Table 2 lists the theoretical maximum adsorption capacity of Pb^{2+} for several adsorption materials reported in the literature, compared with the three biochars in this study. The maximum adsorption capacity of BC1 prepared by pyrolysis of raw sludge is generally lower than that of general modified materials. In contrast, the largest adsorption capacity of BC3 prepared by sludge pyrolysis after K_2FeO_4 conditioning capacity exceeds most materials; only lower than APTES functionalized magnetic biochar and CMC-MMT organic-inorganic hybrid composite.

However, the adsorption pH conditions of these two materials are weakly alkaline and neutral. Under these pH conditions, a large amount of Pb^{2+} may be removed by generating $Pb(OH)_2$ alkaline precipitation, and the surface adsorption of the material itself may be less. The higher the pH, the less Gibbs free energy required to form a metal precipitate [27], and the faster the kinetic process of surface precipitation. Consequently, the above factors make it easier to remove heavy metals under high pH conditions. Therefore, the removal effect of BC2 and BC3 under acidic conditions seems to be excellent among similar adsorbent materials.

3.3. Adsorption mechanism

3.3.1. Ion exchange

In order to explore the ion exchange effect in the process of lead adsorption, the concentrations of 24 major cation ions (As, Al, Ba, Be, Bi, B, Cd, Ca, Cr, Co, Cu, Fe, Pb, Li, Mg, Mn, Ni, P, K, Se, Na, Sr, V and Zn) were measured by ICP. Only Ca^{2+} and Mg^{2+} show obvious leaching, while the other 22 elements were not detected. The occurrence of Ca^{2+} and Mg^{2+} in the leaching process may be attributed to the existence of R-O-Me or R-COO-Me functional groups on the surface of biochar (Me represents the central metal atom), or calcium and magnesium precipitate on the surface of biochar. During the Pb^{2+} adsorption process, due to the acidic environment or the relatively stable newly formed precipitates or complexes containing Pb^{2+}, they may dissociate or dissolve [25]. During adsorption, some calcium and magnesium precipitate dissolved at pH = 3, and others exchange ions with Pb^{2+}; thus, Ca^{2+} and

Table 3
Contribution rates of ion exchange for the removal of 100 mg/L Pb^{2+}.

Adsorbent	Pb^{2+} effluent concentration	Ca^{2+} Leaching concentration	Mg^{2+} Leaching concentration	Contribution rate
	$mg \cdot L^{-1}$	$mg \cdot L^{-1}$	$mg \cdot L^{-1}$	%
BC1	75.97	2.18	3.00	5.18
BC2	0.15	8.1	4.79	12.89
BC3	41.16	13.08	5.83	18.91

Mg^{2+} were released into the solution.

Fig. 3 depicts how Ca^{2+} and Mg^{2+} concentrations changed with time (the value has already been deducted the biochar background value of Ca^{2+} and Mg^{2+} leached at pH 3). In the first 5 min, ion exchange occurred rapidly and then slowed down. The exchange capacity of Ca^{2+} and Pb^{2+} is higher than Mg^{2+} and Pb^{2+} for the three biochars in the whole process. According to the effluent concentration of Pb^{2+} and the leaching concentration of Ca^{2+} and Mg^{2+} after 2 h, the contribution rate of ion exchange for the Pb^{2+} removal for the three biochars was calculated (Table 3; See also SM, Text S5 for calculation method).

Compared to BC3, BC2 exhibited greater removal efficiency (100 mg/L Pb^{2+} within 2 h), but lower leaching amounts of Ca^{2+} and Mg^{2+}, so the ion exchange effect of BC3 was more substantial.

### 3.3.2. Functional groups

Sludge-derived biochar contains a large number of free or complex functional groups, such as -COOH, R-OH, and phenolic hydroxyl groups, which can remove Pb^{2+} in the solution through electrostatic attraction or surface complexation, generating humus containing -COO-Me, − R-O-Me, or other functional groups [36,37].

To study the contribution rate of functional group complexation for Pb^{2+} removal, R-COOH and R-OH were blocked by methanol and formaldehyde, respectively, Afterward, the Pb^{2+} adsorption capacity of BC2 and BC3 decreased meaningfully. The contribution rates of functional groups for the removal of 100 mg/L Pb^{2+} are summarized in Table 4. Approximately 79% of Pb^{2+} was removed by BC2, followed by BC3, and the lowest amount was removed by BC1. BC2 had the highest abundance of functional groups, so when they were blocked, the adsorption effect was mostly affected, indicating that functional group complexation is the most robust mechanism in the adsorption process. (See SM, Text S5 for calculation method).

Table 4
Contribution rates of functional groups to the removal of 100 mg/L Pb^{2+}.

Adsorbent	Pb^{2+} effluent concentration (-COOH blocked)	Contribution rate	Pb^{2+} effluent concentration (-OH blocked)	Contribution rate	Total contribution rate
	$mg \cdot L^{-1}$	%	$mg \cdot L^{-1}$	%	%
BC1	84.60	8.63	85.19	9.22	17.85
BC2	41.07	40.92	38.22	38.07	78.99
BC3	62.99	21.83	58.31	17.15	38.98
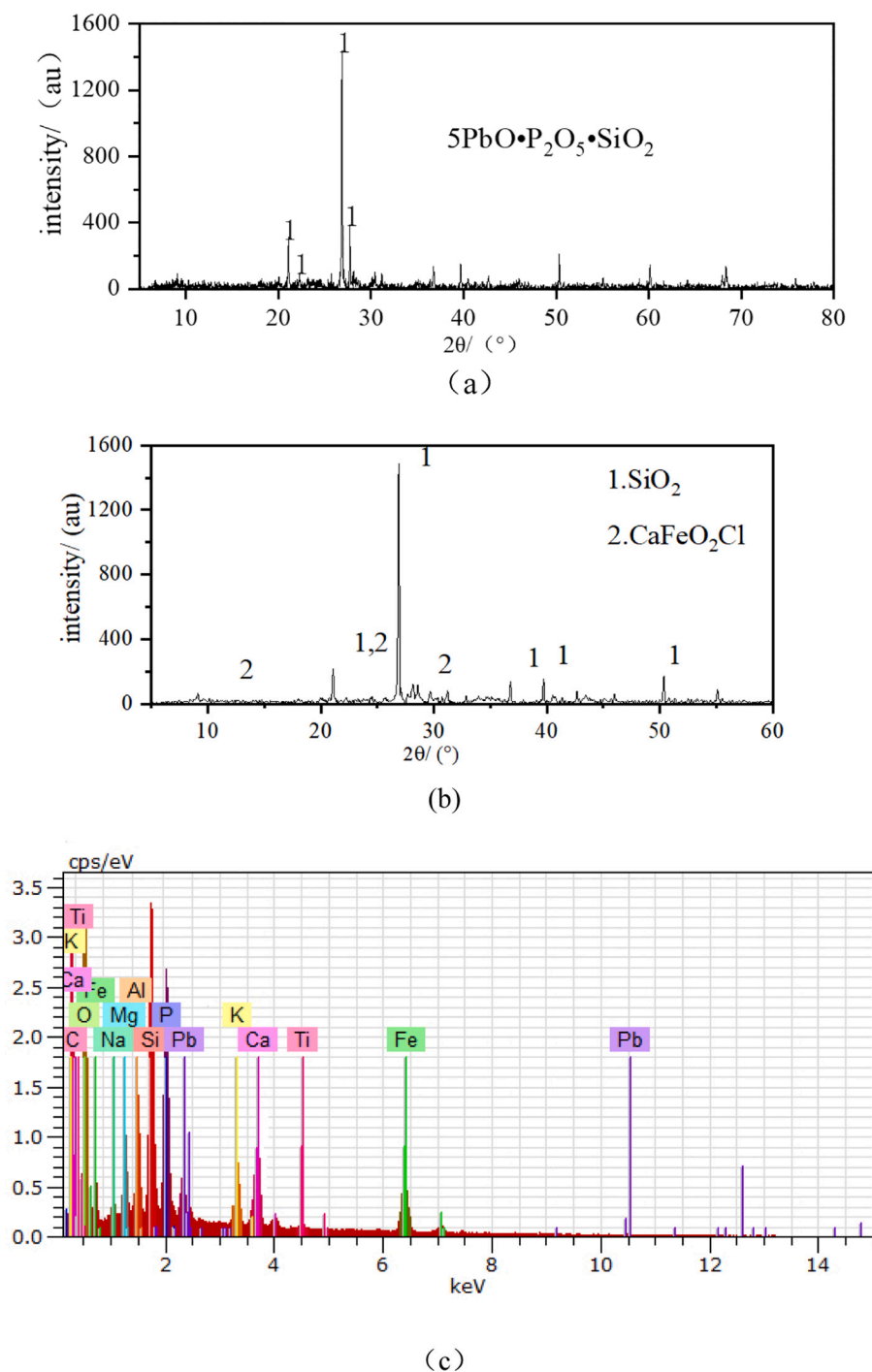
Fig. 4. (a) XRD pattern of BC2 after lead adsorption, (b) XRD pattern of BC2 without adsorption, and (c) EDX spectrum of Pb^{2+}-adsorbed BC2. (Samples prepared at pH 3).
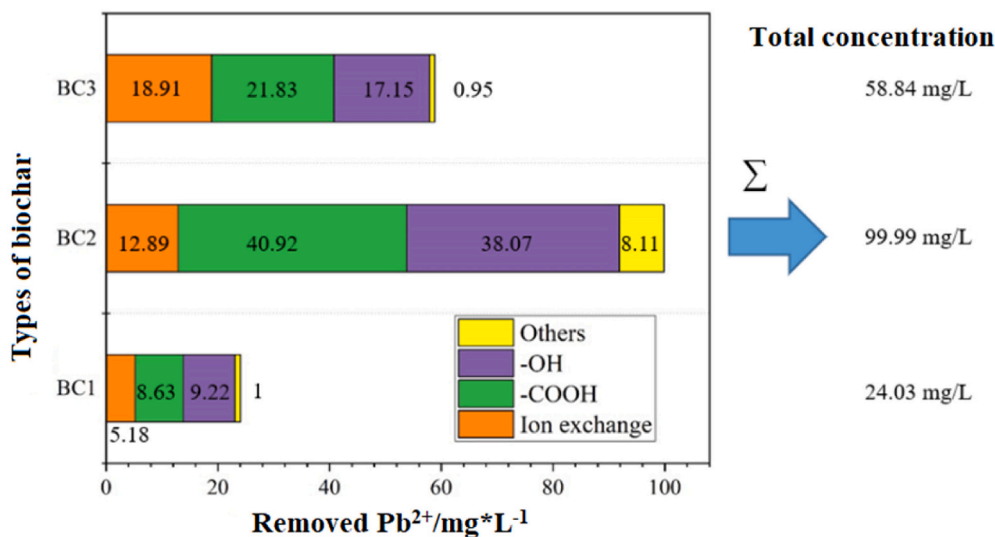
Fig. 5. The contribution rates (%) of each mechanism for the removal of Pb^{2+}.

Table 5
The leached Pb^{2+} for three biochars types.

Biochar	Leaching Pb^{2+}/(mg·L^{-1})	
	Initial Pb^{2+} = 1 mg/L	Initial Pb^{2+} = 75 mg/L
BC1	0.11	12.62
BC2	0.04	0.88
BC3	0.14	5.83

3.3.3. Other effects

Weak alkalinity (pH = 8–9) of the biochar leachate can cause simple alkaline precipitation, coprecipitation, or other chemical effects. As a carbon-based material, sludge-derived biochar with a specific porosity can lead to simple physical adsorption.

XRD of three biochar samples after adsorbing 100 mg/L Pb^{2+} was measured to understand the effect of chemical precipitation, and the patterns were similar (Fig. 4a shows BC2 for analysis). Before adsorption, a large amount of silica existed (Fig. 4b). After adsorption, the silica peak disappeared in the spectrum, and an apparent $5PbO \cdot P_2O_5 \cdot SiO_2$ peak appeared. SEM-EDX was used to scan the biochars that adsorbed Pb^{2+} to determine the Pb^{2+}-enriched area on the biochar surface, and then the energy spectrum was analyzed in this area to explore the elemental composition and approximate content as shown in Fig. 4c and SM, Fig. S4. The enrichment of P, Si, and Pb in the precipitation area verified the existence of $5PbO \cdot P_2O_5 \cdot SiO_2$. This new substance may be the product of the coprecipitation reaction of Pb^{2+}, activated silica, and phosphate in the biochar since studies have confirmed that the total phosphorus in sludge-derived biochar is up to 2.4% [25]. The Pb—Si coprecipitation reaction has also been reported [38].

Other forms of Pb precipitation, including $Pb(OH)_2$, $PbCO_3$, β-$Pb_9(PO_4)_6$, $Pb_5(PO_4)_3Cl$, and $Pb_3(CO_3)_2(OH)_2$, have been reported in the literature concerning Pb^{2+} adsorption with other biochars [39,40], but they were not detected in this study. Possible reasons are compatibilization of the component anions, reaction time, and solution pH, which caused these precipitates to be amorphous [41].

By subtracting the ion exchange and functional group removal from the total amount of Pb^{2+}, the removal volume of other effects, including chemical precipitation and simple physical adsorption, can be obtained.

The contribution rate (%) comparison of each mechanism and the removal quantity sum for each biochar is summarized in Fig. 5.

3.4. Leaching experiment

When the three kinds of biochar adsorbed 1 mg·L^{-1} Pb^{2+}, the leached Pb^{2+} (Table 5) was lower than 0.25 mg·L^{-1}, which can meet the Chinese national "Standard for Pollution Control on the Landfill Site of Municipal Solid Waste" (GB 16889-2008).

As the initial concentration of Pb^{2+} increased, the concentration of Pb^{2+} in the leachate rose. Among them, BC1 has the worst effect on removing 75 mg·L^{-1} Pb^{2+}, but it leaches the highest concentration of Pb^{2+}. BC2 can entirely remove 75 mg·L^{-1} Pb^{2+}, and the leaching concentration is the lowest. BC3 can remove 80% of Pb^{2+}, revealing that following K_2FeO_4 conditioning, the biochar's adsorption stability is greatly improved compared with the original sludge-derived biochar. The BC2 leaching toxicity can still meet the 1.2 mg·L^{-1} limit for adsorbing high concentration Pb^{2+}, specified in the national "Standard for Pollution Control on the Hazardous Waste Landfill" (GB 18598-2019).

4. Conclusion

Three types of sludge-derived biochar were prepared from the original sludge, K_2FeO_4 conditioned sludge, and acidified+K_2FeO_4 conditioned sludge. The three biochars were utilized to adsorb Pb^{2+} in water. Experiments show that the Pb^{2+} concentration in the adsorption water of biochar adjusted by acidification + K_2FeO_4 is lower than the detection limit of ICP-MS (<0.06 μg). The removal mechanism of Pb^{2+} by biochar in water is divided into three parts: 1) ion exchange with Ca^{2+} and Mg^{2+}; 2) surface complexation of free COOH and OH; and 3) chemical precipitation or possible physical adsorption. Biochar prepared from sludge conditioned by K_2FeO_4 contains added functional groups. The complexation of functional groups has been strengthened, leading to greater removal of Pb^{2+}. Therefore, this research makes it possible to reduce sludge and develop a new type of adsorbent to treat Pb^{2+} in water.

Declaration of Competing Interest

The authors declare that they have no known competing financial interests or personal relationships that could have appeared to influence the work reported in this paper.

Acknowledgements

Appendix A. Supplementary data

Supplementary data to this article can be found online at https://doi.org/10.1016/j.colcom.2021.100417.

References

[1] W. Fang, et al., Overview of key operation factors and strategies for improving fermentative volatile fatty acid production and product regulation from sewage sludge, J. Environ. Sci. 87 (2020) 93–111.

[2] J. Racek, et al., Biochar - recovery material from pyrolysis of sewage sludge: a review, Waste Biomass Valorization 11 (7) (2020) 3677–3709.

[3] Z. Lei, et al., Effects of variations of extracellular polymeric substances and soluble microbial products on activated sludge properties during anaerobic storage, Environ. Technol. 28 (5) (2007) 529–544.

[4] W. Yu, et al., Effect of sludge retention on UF membrane fouling: the significance of sludge crystallization and EPS increase, Water Res. 83 (2015) 319–328.

[5] W. Zhang, et al., Novel pectin based composite hydrogel derived from grapefruit peel for enhanced Cu(II) removal, J. Hazard. Mater. 384 (2020).

[6] Y.-Y. Wang, et al., Ammonium citrate-modified biochar: an adsorbent for La(III) ions from aqueous solution, Colloids Surf. A-Physicochem. Eng. Asp. 509 (2016) 550–563.

[7] F. Barbier, G. Duc, M. Petit-Ramel, Adsorption of lead and cadmium ions from aqueous solution to the montmorillonite/water interface, Colloids Surfaces A-Physicochem. Eng. Asp. 166 (1–3) (2000) 153–159.

[8] C.-V. Gherasim, J. Krivcik, P. Mikulasek, Investigation of batch electrodialysis process for removal of lead ions from aqueous solutions, Chem. Eng. J. 256 (2014) 324–334.

[9] G. Li, et al., Amide-based covalent organic frameworks materials for efficient and recyclable removal of heavy metal lead (II), Chem. Eng. J. 370 (2019) 822–830.

[10] H. Demey, et al., Evaluation of torrefied poplar-biomass as a low-cost sorbent for lead and terbium removal from aqueous solutions and energy co-generation, Chem. Eng. J. 361 (2019) 839–852.

[11] C. Wang, H. Wang, Y. Cao, Pb(II) sorption by biochar derived from *Cinnamomum camphora* and its improvement with ultrasound-assisted alkali activation, Colloids Surf. A-Physicochem. Eng. Asp. 556 (2018) 177–184.

[12] J.H. Park, et al., Comparison of heavy metal immobilization in contaminated soils amended with peat moss and peat moss-derived biochar, Environ. Sci.-Process. Impacts 18 (4) (2016) 514–520.

[13] M. Meepho, W. Sirimongkol, J. Ayawanna, Samaria-doped ceria nanopowders for heavy metal removal from aqueous solution, Mater. Chem. Phys. 214 (2018) 56–65.

[14] X. Huang, et al., Synthesis of amino-functionalized magnetic aerobic granular sludge-biochar for Pb(II) removal: adsorption performance and mechanism studies, Sci. Total Environ. 685 (2019) 681–689.

[15] J. Hu, et al., Using a strong chemical oxidant, potassium ferrate (K2FeO4), in waste activated sludge treatment: a review, Environ. Res. 188 (2020).

[16] L. Zheng, Y. Deng, Settleability and characteristics of ferrate(VI)-induced particles in advanced wastewater treatment, Water Res. 93 (2016) 172–178.

[17] J. Wu, et al., A novel sewage sludge biochar and ferrate synergetic conditioning for enhancing sludge dewaterability, Chemosphere 237 (2019).

[18] W. Li, et al., Co-treatment of potassium ferrate and ultrasonication enhances degradability and dewaterability of waste activated sludge, Chem. Eng. J. 361 (2019) 148–155.

[19] Y. Wu, et al., Combined sludge conditioning of micro-disintegration, floc reconstruction and skeleton building (KMnO4/FeCl3/Biochar) for enhancement of waste activated sludge dewaterability, J. Taiwan Inst. Chem. Eng. 74 (2017) 121–128.

[20] J.P. Chen, L. Yang, Study of a heavy metal biosorption onto raw and chemically modified Sargassum sp via spectroscopic and modeling analysis, Langmuir 22 (21) (2006) 8906–8914.

[21] J.L. Gardeatorresdey, et al., Effect of chemical modification of algal carboxyl groups on metal ion binding, Environ. Sci. Technol. 24 (9) (1990) 1372–1378.

[22] B. Chen, Z. Chen, Sorption of naphthalene and 1-naphthol by biochars of orange peels with different pyrolytic temperatures, Chemosphere 76 (1) (2009) 127–133.

[23] J.-H. Yuan, R.-K. Xu, H. Zhang, The forms of alkalis in the biochar produced from crop residues at different temperatures, Bioresour. Technol. 102 (3) (2011) 3488–3497.

[24] R.M. Novais, et al., Red mud-based inorganic polymer spheres bulk-type adsorbents and pH regulators, Mater. Today 23 (2019) 105–106.

[25] H. Lu, et al., Relative distribution of Pb2+ sorption mechanisms by sludge-derived biochar, Water Res. 46 (3) (2012) 854–862.

[26] I.A.W. Tan, A.L. Ahmad, B.H. Hameed, Adsorption of basic dye on high-surface-area activated carbon prepared from coconut husk: equilibrium, kinetic and thermodynamic studies, J. Hazard. Mater. 154 (1–3) (2008) 337–346.

[27] Y.J. Yin, et al., The importance of organic matter distribution and extract soil: solution ratio on the desorption of heavy metals from soils, Sci. Total Environ. 287 (1–2) (2002) 107–119.

[28] Q. He, et al., Preconcentration of cu(II), Fe(III) and Pb(II) with 2-((2-aminoethylamino)methyl)phenol-functionalized activated carbon followed by ICP-OES determination, J. Hazard. Mater. 175 (1–3) (2010) 710–714.

[29] H. Ge, J. Du, Selective adsorption of Pb(II) and Hg(II) on melamine-grafted chitosan, Int. J. Biol. Macromol. 162 (2020) 1880–1887.

[30] O.S. Lawal, et al., Equilibrium, thermodynamic and kinetic studies for the biosorption of aqueous lead(II) ions onto the seed husk of *Calophyllum inophyllum*, J. Hazard. Mater. 177 (1–3) (2010) 829–835.

[31] E.C. Nnadozie, P.A. Ajibade, Adsorption, kinetic and mechanistic studies of Pb(II) and Cr(VI) ions using APTES functionalized magnetic biochar, Microporous Mesoporous Mater. 309 (2020).

[32] H. Zhang, et al., Mechanism of carboxymethyl chitosan hybrid montmorillonite and adsorption of Pb(II) and Congo red by CMC-MMT organic-inorganic hybrid composite, Int. J. Biol. Macromol. 149 (2020) 1161–1169.

[33] J. Zhang, et al., Sludge-based biochar activation to enhance Pb(II) adsorption, Fuel 252 (2019) 101–108.

[34] J. Liu, et al., Resource utilization of swine sludge to prepare modified biochar adsorbent for the efficient removal of Pb(II) from water, J. Clean. Prod. 257 (2020).

[35] Y. Xue, et al., Pyrolysis of sewage sludge by electromagnetic induction: biochar properties and application in adsorption removal of Pb(II), Cd(II) from aqueous solution, Waste Manag. 89 (2019) 48–56.

[36] J.F.d.S.S. Costa, et al., Application of the Nernst-Planck approach to lead ion exchange in Ca-loaded *Pelvetia canaliculata*, Water Res. 44 (13) (2010) 3946–3958.

[37] N. Zhou, et al., In situ modification provided by a novel wet pyrolysis system to enhance surface properties of biochar for lead immobilization, Colloids Surf. A-Physicochem. Eng. Asp. 570 (2019) 39–47.

[38] M. Iqbal, A. Saeed, S.I. Zafar, FTIR spectrophotometry, kinetics and adsorption isotherms modeling, ion exchange, and EDX analysis for understanding the mechanism of Cd2+ and Pb2+ removal by mango peel waste, J. Hazard. Mater. 164 (1) (2009) 161–171.

[39] J.A. Ryan, et al., Formation of chloropyromorphite in a lead-contaminated soil amended with hydroxyapatite, Environ. Sci. Technol. 35 (18) (2001) 3798–3803.

[40] X. Cao, et al., Dairy-manure derived biochar effectively sorbs lead and atrazine, Environ. Sci. Technol. 43 (9) (2009) 3285–3291.

[41] A. Swiatkowski, et al., Influence of the surface chemistry of modified activated carbon on its electrochemical behaviour in the presence of lead(II) ions, Carbon 42 (15) (2004) 3057–3069.